ACTIVE VIBRATION CONTROL IN A ROTOR SYSTEM USING AN ELETROMAGNETIC ACTUATOR WITH H_∞ NORM

Edson Hideki Koroishi, koroishi@mecanica.ufu.br[1]
Aldemir Aparecido Cavalini Júnior, aacjunior@mecanica.ufu.br[1]
Valder Steffen, Jr, vsteffen@mecanica.ufu.br[1]
Jarir Mahfoud, jarir.mahfoud@insa.lyon.fr[2]

[1] Federal University of Uberlândia (UFU) - School of Mechanical Engineering - Campus Santa Mônica, Av. João Naves de Ávila 2121, Bloco 1M, Uberlândia, MG, Brazil, ZIP CODE 38400-902, www.femec.ufu.br
[2] *Lyon University, LAMCOS, INSA de Lyon, 20, Av. Albert Einstein, 69629 Villeurbanne, France*

Abstract. *In recent years, a number of new methods dedicated to acoustic and vibration attenuation have been developed and proposed to handle several problems in engineering. This is due to the demand for better performance and safely operation of mechanical systems. There are various types of actuators available. The present contribution is dedicated to the electromagnetic actuator (EMA). EMA uses electromagnetic forces to support the rotor without mechanical contact. Due to the size of the system model, it was necessary to reduce the model of the rotating system. For this aim the balanced realization technique was used to organize the modes of the system so that the main modes (with respect to the dynamic behavior of the system) are considered. The control design for the discrete state-space formulation is carried out through a feedback technique and the H_∞ norm was solved by using Linear Matrix Inequalities (LMI). State observers were used to estimate some states of the system since it is not practical from the experimental view point to measure all the states of the system. The design of the state observers was performed by using LMIs. Finally, simulation results demonstrate the effectiveness of the methodology conveyed.*

Keywords*: Active Vibration Control, Electromagnetic Actuator, State Observer, H_∞ norm, LMIs*

1. INTRODUCTION

Currently, an increase of research works in engineering dedicated to the development of active vibration control techniques (AVC) is observed. This effort is stimulated by the necessity of lighter structures associated to higher operational performance and smaller operating costs (Bueno, 2007). In the last decades, the methodologies of AVC have received significant contributions, due particularly to the advances in the digital processing of signals and new methodologies of control as can be seen in Fuller et al (1996), Hansen et al (1997), Gawronski (1998) and Juang et al (2001). Some of these contributions have caused deep impact in aerospace and robotic applications (Liu et al, 2000).

In the context of rotor dynamics, Saldarriaga (2007) classifies the AVC techniques in two major categories: the active vibration control that consists in the application of lateral forces to oppose the forces caused by the vibration, and the active balancing that consists in the redistribution of the mass along the rotor with the intervention of actuators, so that the rotor can be balanced. Simões (2006) developed an AVC methodology for flexible rotors by using piezoelectric stack actuators. In this work, the optimal control is based on the Linear Quadratic Regulator approach aiming at attenuating the first 4 vibration modes of the system.

In terms of rotating machines, another important AVC methodology uses Active Magnetic Bearings. The AMB is a feedback mechanism that supports a spinning shaft by levitating it in a magnetic field (Koroishi et al, 2009). Figure 1 shows one quadrant of a radial AMB consisting of a position sensor, a controller, a power amplifier and an electromagnetic actuator. For its operation, the sensor measures the relative position of the shaft and the measured signal is sent to the controller where it is processed. Then, the signal is amplified and fed as electric current into the coils of the magnet, generating an electromagnetic field that keeps the shaft in a desired position. The strength of the magnetic field depends both on the air gap between the shaft and the magnet and the dynamics of the system including the design of the controller.

The basic idea regarding the electromagnetic actuator (EMA) is similar to the AMB. In this context, the goal of this work is to develop an AVC methodology using EMA. The controller is obtained by using the H_∞ norm. For model reduction purposes the well known pseudo-modal technique was used. State observers were designed by using LMIs (Linear Matrix Inequalities).

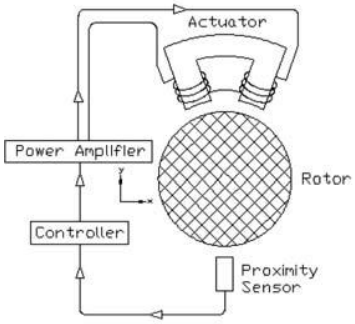

Figure 1. Magnetic levitation principle (Kasarda et al, 2007).

2. FLEXIBLE ROTORS

The dynamic response of the considered mechanical system can be modeled by using principles of variational mechanics, namely the Hamilton`s principle. For this aim, the strain energy of the shaft and the kinetic energies of the shaft and discs are calculated. An extension of Hamilton`s principle makes possible to include the effect of energy dissipation. The parameters of the bearings are considered in the model by using the principle of the virtual work. For computation purposes, the finite element method is used to discretize the structure so that the energies calculated are concentrated at the nodal points. Shape functions are used to connect the nodal points. To obtain the stiffness of the shaft the Timoshenko`s beam theory was used and the cross sectional area was updated as proposed by Hutchison, 2001. The model obtained as described above is represented mathematically by the set of differential equations (Lalanne, 1997) given by Eq. (1).

$$[M]\{\ddot{x}(t)\}+\left[C_b+\dot{\phi}C_g\right]\{\dot{x}(t)\}+\left[K+\dot{\phi}K_g\right]\{x(t)\}=\{F_u(t)\}+\{F_{EMA}(t)\} \tag{1}$$

where $\{x(t)\}$ is the vector of generalized displacements; $[M]$, $[K]$, $[C_b]$, $[C_g]$ e $[K_g]$ are the well known matrices of inertia, stiffness, bearing viscous damping (that may include proportional damping), Coriolis (with respect to the speed of rotation), and the effect of the variation of the rotation speed; $\dot{\phi}$ is the time-varying angular speed, and $\{F_u(t)\}$ and $\{F_{EMA}(t)\}$ are the forces due to the unbalance and to the electromagnetic actuator, respectively.

The finite element model considers 4 d.o.f. per node, namely two displacements (along the directions x and z) and two rotations (around the axes x and z), respectively. The model was discretized according to 43 nodes as shown in the Fig. 2b. The ball bearings (B_1) are located at the nodes # 4 and # 5 and the bearing containing the electromagnetic actuator (B_2) is placed at the node #39. The first disc (D_1) is placed between the nodes #12 and #15; the second disc (D_2) is located between the nodes #29 and #31. Finally, concentrated masses were included in the model at the position of the bearings and at the coupling between the shaft and the motor.

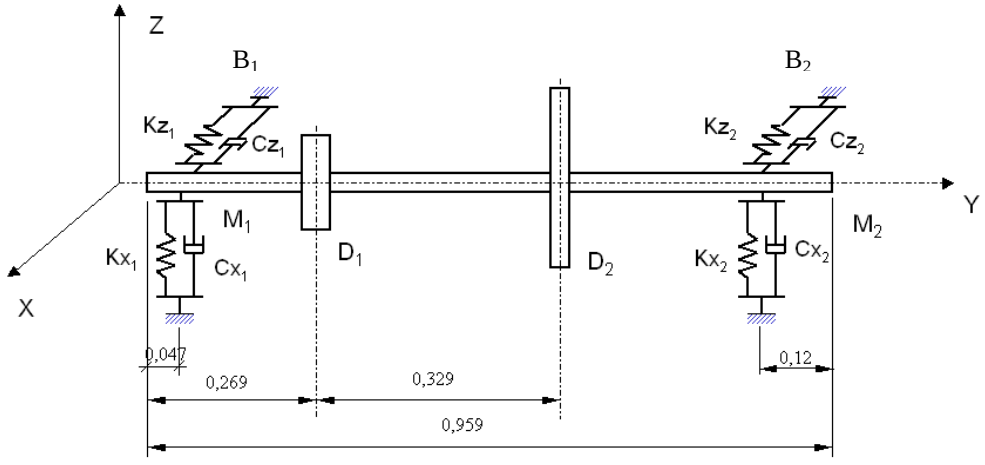

Figure 2. Scheme of rotor (Simões, 2006).

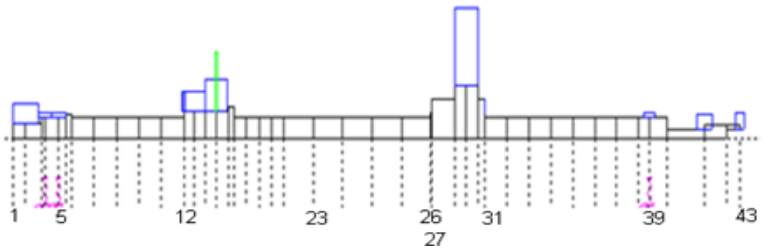

Figure 3. Discretização do modelo de elementos finitos (Simões, 2006).

The Tab. (1) shows the physical properties of the rotor.

Table 1. Physical characteristics of rotor-bearing system.

Characteristic	Value
Rotor	
Mass of shaft (kg)	9.690
Mass of disc D_1 (kg)	2.032
Mass of disc D_2 (kg)	10.61
Thickness of D_1 (m)	0.029
Thickness of D_2 (m)	0.030
Diameter of shaft (m)	0.040
Bearings	
k_{x1} (N/m)	$1.16754X10^8$
k_{z1} (N/m)	$1.65140X10^8$
k_{x2} (N/m)	$1.40860X10^6$
k_{z2} (N/m)	$1.43410X10^6$
C_{x1}, C_{x2}, C_{z1}, C_{z2} (N.s/m)	280, 120, 300, 120

Other properties used for the shaft are the following: Elastic or Young Modulus (E) = 210 GN/m^2, density = 7800Kg/m^3 and Poison Coefficient = 0.3.

2.1. Pseudo-Modal Method

In practical cases, the use of a larger number of degrees of freedom (dof) results in a high computational cost without significant influence in the calculation of the lower modes. In this case it is recommended to reduce the size of the model. For this aim the well-known pseudo-modal method is applied. The reduction is achieved by changing from the physical coordinates $\{x(t)\}$ to modal coordinates $\{q(t)\}$ (Simões et al, 2006):

$$\{x(t)\} = [\phi]\{q(t)\} \tag{2}$$

where $[\phi]$ is the modal basis that contains the *m* first modes of the non-gyrocopic conservative associated system.

From Eq. (1) a modal basis is defined by the solutions of:

$$[M]\{\ddot{x}(t)\} + [K^*]\{x(t)\} = 0 \tag{3}$$

where $[K^*]$ is the stiffness matrix, obtained from $[K]$, in which the terms introduced by the bearings vanish.

The *n* first modes $\phi_1, \ldots, \phi_n$ form the pseudo-modal matrix:

$$[\phi] = [\phi_1, \ldots, \phi_n] \tag{4}$$

Using the modal basis given by Eq. (4), the reduced model can be represented by:

$$[\phi]^T [M][\phi]\{\ddot{q}\} + [\phi]^T [C][\phi]\{\dot{q}\} + [\phi]^T [K][\phi]\{q\} = [\phi]^T \{F(t)\} \tag{5}$$

3. ELETROMAGNETIC ACTUATOR

The electromagnetic actuator introduces forces that are inversely proportional to the square of the gap. For each coil, the force is given by Eq. (6), Damien, 2003.

$$F_{EMA} = \frac{N^2 I^2 \mu_0 af}{2\left((e \pm \delta) + \frac{b+c+d-2a}{\mu_r} \right)^2} \tag{6}$$

The parameters that define the geometry of the coils (*a*, *b*, *c*, *d* e *f*) are shown in the Fig. (4); μ_0 e μ_r are the magnetic permeability in the vacuum and the relative permeability of the material, respectively. μ_r is determined experimentally. The gap is given by *e*; δ is the variation of the gap due to the vibration of the rotor at the position of the electromagnetic actuator.

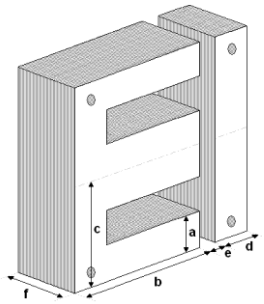

Figure 4. Ferromagnetic circuit.

The parameters of the coil are described in Tab. (2).

Table 2. Parameters of the coil (Morais et al, 2009).

μ_0 (H/m)	1.2566e-06
μ_r (H/m)	700
N (spires)	278
a (mm)	21
b (mm)	84
c (mm)	63
d (mm)	21
f (mm)	42
e (mm)	1.5

4. LINEAR MATRIX INEQUALITIES (LMIs)

LMIs have been used in the analysis of dynamical systems for more than 100 years. They date from 1890, when Aleksandr Mikhailovich Lyapunov presented his original work, thus introducing the well-known Lyapunov Theory (Boyd et al, 1994). He demonstrated that the differential equation:

$$\dot{x}(t) = Ax(t) \tag{7}$$

is stable (all the trajectories converge to zero), if and only if there is a positive-definite matrix P such that:

$$A^T P + PA > 0 \tag{8}$$

The inequality given by Eq. (8) is known as the Lyapunov inequality.

Currently, LMIs have been the object of study by many important researchers around of the world: the control of continuous and discrete systems in the time domain, optimal control, and robust control (Van Antwerp et al, 2000 and Silva et al, 2000), model reduction (Assunção, 2000), control of nonlinear systems, theory of robust filters (Palhares, 2000), and detection, location and quantification of faults (Abdalla et al, 2000 and Wang et al, 2007).

4.1. Decay Rate

The decay rate, known as the largest Lyapunov exponent, is defined as being the largest α , $\alpha>0$, such that (Boyd *et al*, 1994):

$$\lim_{t\to\infty} e^{\alpha t}\left\|x(t)\right\| = 0 \tag{9}$$

for all trajectories given by *x*. For the stability to occur, a positive decay is necessary.

The decay rate is a parameter used in the control theory, which is one of the design constraints. For example, Silva *et al* (2004) used the decay rate as a design constraint in their works, where they presented a methodology for active vibration control with robustness requirements.

4.2. State Observers using LMIs

A state observer is defined by:

$$\begin{aligned}\left\{\dot{\bar{x}}(t)\right\} &= [A]\left\{\bar{x}(t)\right\} + [B]\{u(t)\} + [L]\left(\{y(t)\} - \left\{\bar{y}(t)\right\}\right)\\ \left\{\bar{y}(t)\right\} &= [C_{me}]\left\{\bar{x}(t)\right\}\end{aligned} \tag{10}$$

where:

$[A] \in R^{nxn}$ is the dynamical matrix;

$[B] \in R^{nxp}$ is the input matrix;

$[C_{me}] \in R^{kxn}$ is the measure matrix;

n is the order of the system, *p* the number of inputs $\{u(t)\}$, *k* the number of outputs $\{y(t)\}$.

$[L]$ is the observer matrix;

$\left\{\bar{y}(t)\right\}$ is the output of the observer;

$\left\{\bar{x}(t)\right\}$ is the state vector of the observer.

In this case, the study of stability of the state observer is attained by using the following LMIs:

$$\begin{aligned}&[P_{lmi}]([A]-[L][C_{me}]) + ([A]-[L][C_{me}])^T[P_{lmi}] < 0\\ &[P_{lmi}] > 0\end{aligned} \tag{11}$$

where:

$[P_{lmi}] = [P_{lmi}]^T$;

$[A]-[L][C_{me}]$ is the observability matrix.

After manipulations it is possible to obtain:

$$[P_{lmi}][A]-[P_{lmi}][L][C_{me}]+[A]^T[P_{lmi}]-[C_{me}]^T[L]^T[P_{lmi}] < 0 \tag{12}$$

Multiplying both sides of Eq. (11) by P^{-1}, the following equation is obtained:

$$[A][P_{lmi}]^{-1}-[L][C_{me}][P_{lmi}]^{-1}+[P_{lmi}]^{-1}[A]^T-[P_{lmi}]^{-1}[C_{me}]^T[L]^T < 0 \tag{13}$$

Defining $[X_{lmi}] = [P_{lmi}]^{-1}$ and $[G] = [P_{lmi}]^{-1}[L] = [X_{lmi}][L]$, one obtains:

$$[A][X_{lmi}]+[X_{lmi}][A]^T-[G][C_{me}]-[C_{me}]^T[G]^T>0$$
$$[X_{lmi}]>0 \tag{14}$$

where $[X_{lmi}]$. Note that $[P_{lmi}]^{-1}$ exists, since $[P_{lmi}]>0$; in other words all the eigenvalues of $[P_{lmi}]$ are greater than zero.

Considering the decay rate:

$$[A][X_{lmi}]+[X_{lmi}][A]^T-[G][C_{me}]-[C_{me}]^T[G]^T+2\alpha[X_{lmi}]>0$$
$$[X_{lmi}]>0 \tag{15}$$

The gain of the state observer is given by:

$$[L]=[X_{lmi}]^{-1}[G] \tag{16}$$

4.3. H_∞ Norm

Boyd *et al* (1994) showed how to calculate de norm H_∞ by using LMIs. The norm H_∞ can be solved by using the following optimization convex problem:

$$\begin{aligned} &\|G\|_\infty = \min \mu \\ &\text{subject to } \begin{bmatrix} A^TP+PA+C^TC & PB \\ B^TP & -\mu \end{bmatrix} < 0 \\ &P>0, \mu>0 \end{aligned} \tag{17}$$

where μ is a scalar.

5. RESULTS AND DISCUSSION

The control strategy is shown in Fig. (5).

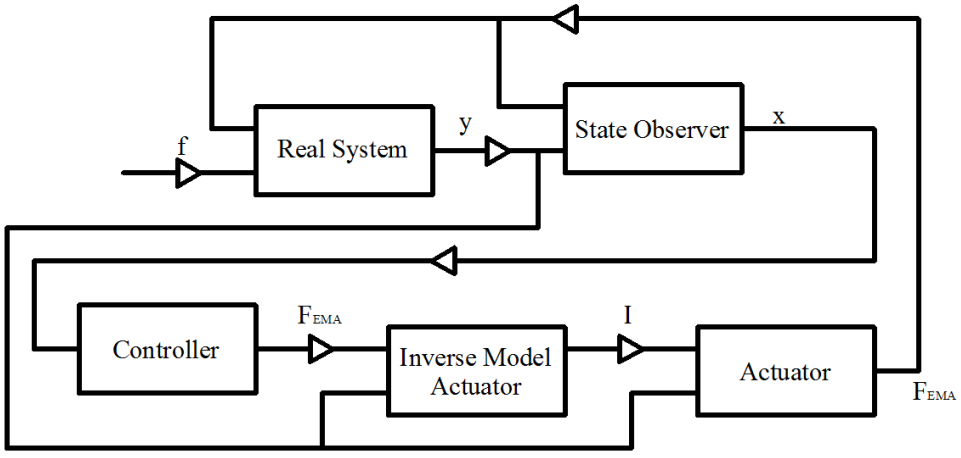

Figure 5. Control strategy.

First, the position of the poles was studied aiming at analyzing the stability of the system. Obviously, the real part of the poles should be negative. The Fig. (6) shows the Pole-Zero map corresponding both to the uncontrolled and controlled systems.

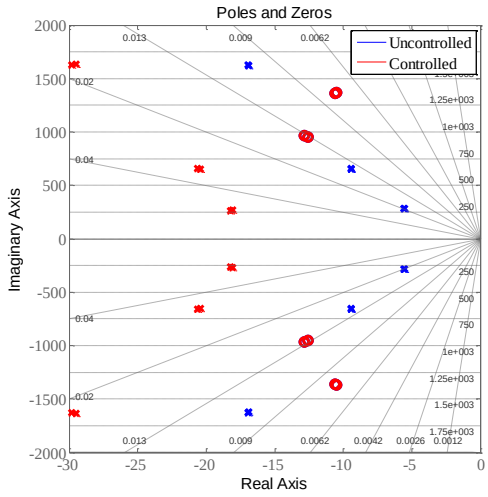

Figure 6. Pole-Zero Map.

As can be seen in Fig. (6) the controlled system presents a larger stability margin than the uncontrolled system, since the corresponding poles are most left in the real axis.

In the following the FRF (Function Response in Frequency) of the system was analyzed by applying an impulse force along the two control directions *x* and *z* as shown in the Fig. 6. Each direction was analyzed separately. It is worth mentioning that the 6 first modes of the system were considered. These modes correspond to 3 in the each direction. It is observed in Fig. (7) that the two FRFs are very similar (along the *x* and *z* directions, respectively). Since the stiffness of the bearings are very close in the *x* and *z* directions.

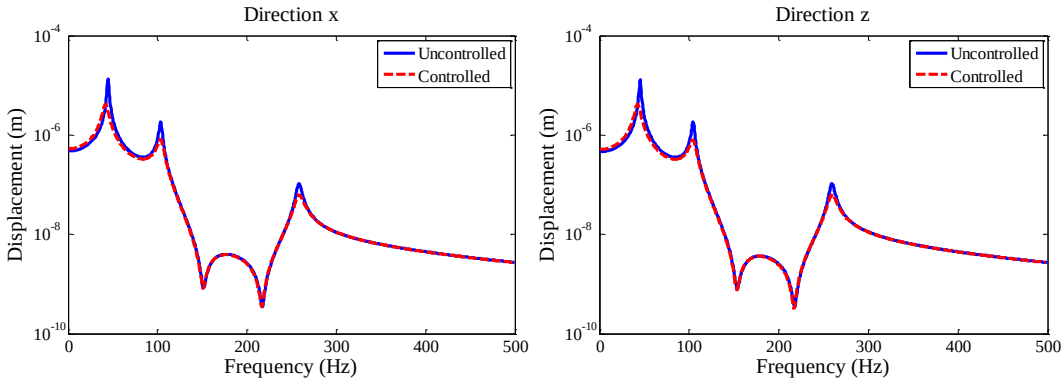

Figure 7. Frequency response functions.

The Tab. (3) shows the percentage amplitude reduction of the considered modes.

Table 3. Comparison of the FRFs peaks of the controlled and uncontrolled systems.

Direction *x*			
Mode	Uncontrolled	Controlled	Reduction (%)
1	1.3301e-5	4.1643e-6	68.69
2	1.8376e-6	8.0917e-7	55.97
3	1.0642e-7	6.1356e-8	42.35
Direction *z*			
1	1.2844e-5	4.1511e-6	67.68
2	1.8353e-6	8.0177e-7	56.31
3	1.0573e-7	6.1749e-8	41.60

Now the rotor behavior is analyzed in the time domain. In this case the unbalance in disk #2 was considered to be *50 g.cm*, located at the node # 29. The displacement signals were measured at this same node. It is important to say that the EMA actuated only when the system displacement were larger than 1e-4 m. In the first analysis a rotation speed of *3000*

rpm (above the first two critical speeds of the system: *2677 rpm* and *2722 rpm*) was considered. The Fig. (8) shows the displacements along the *x* and *z* directions.

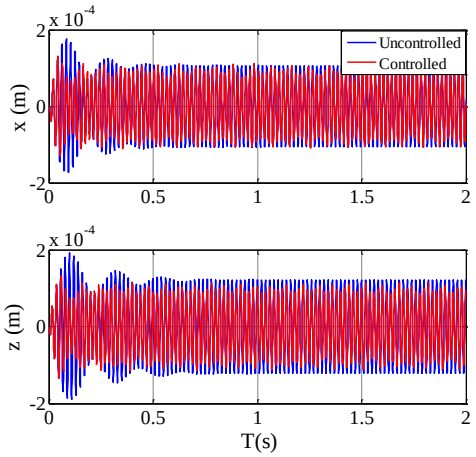

Figure 8. Displacement: rotation 3000 rpm.

For the rotation of 3000 rpm an insignificant reduction in the amplitude of the displacements is observed as a result of the control. At this rotation the system is operating far from the critical speeds. Then the rotation speed was changed to *2700 rpm*, in between the first two critical speeds, and the corresponding results are depicted in the Figure (9).

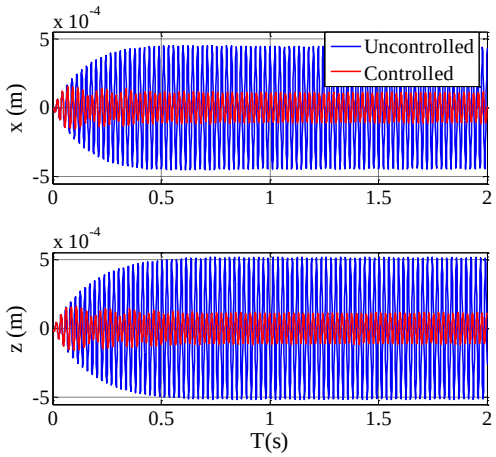

Figure 9. Displacement: rotation 2700 rpm.

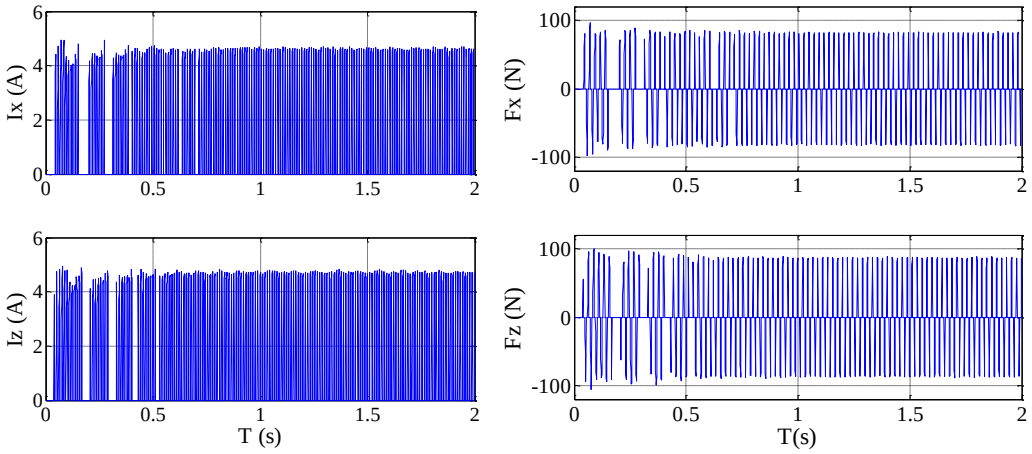

Figure 10. Electrical current and electromagnetic force: rotation 2700 rpm.

Figure (9) demonstrates the efficiency of the controller as characterized by a significant reduction in the amplitudes of the time responses. The last analysis is a run-up test. In this case, the system is accelerating from 0 to 5000 rpm. The results are shown in Fig. (11).

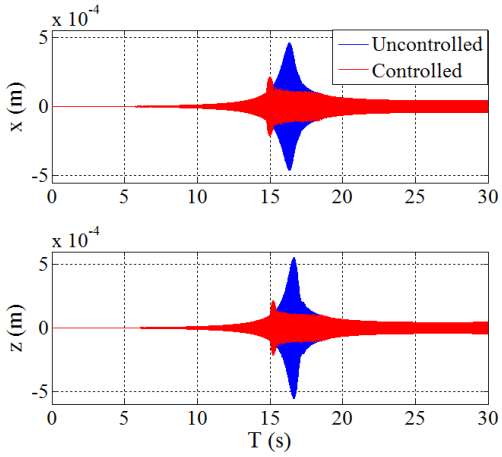

Figure 11. Displacement and electromagnetic actuator: rotation 2700 rpm.

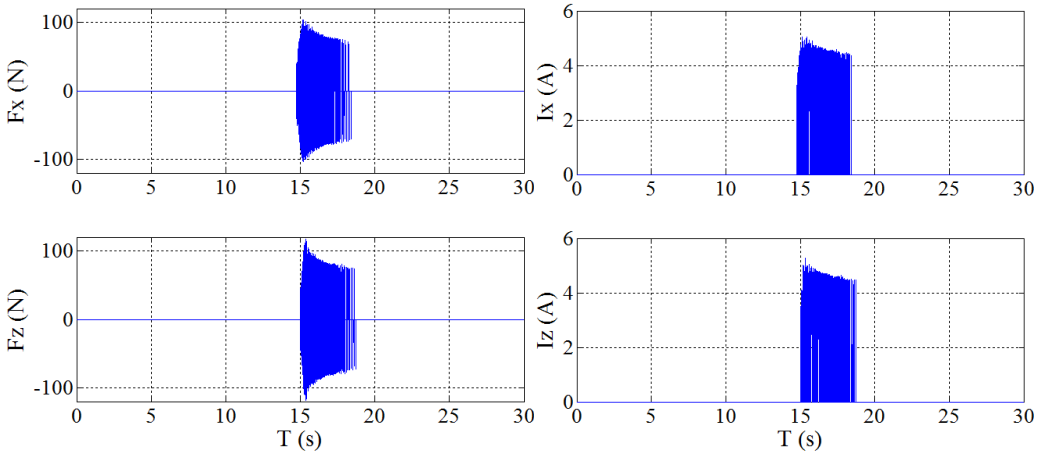

Figure 12. Electrical current and electromagnetic force: rotation 2700 rpm.

Analyzing the results shown in the Figs. (11) and (12), the efficiency of the control in the run-up test is observed. Figure (10) shows the moment in which the actuator is powered (near *15s*). The system was controlled when crossing its critical speed. The Figs. (11) and (12) demonstrates that it is sufficient to turn the actuator on only when the system displacement is larger than a given predefined value.

6. CONCLUSION

In this paper, an active vibration control strategy was proposed by using an electromagnetic actuator. LMIs have been used to obtain the gain of the state observer and also for the resolution of the H_∞ norm.

The results show the effectiveness of the H_∞ norm control both in the time and frequency domains. It can be observed that the controlled system is more stable than the uncontrolled one. The system was controlled in both *x* and *z* directions.

7. ACKNOWLEDGEMENTS

The authors are thankful to the Brazilian Research Agencies FAPEMIG, CNPq and CAPES for the financial support to this work through the INCT-EIE.

8. REFERENCES

Abdalla, M.O.; Zimmerman, D.C.; Grigoriadis, K.M., 2000, “Reduce Optimal Parameter Update in Structural Systems Using LMIs”, American Control Conference, Chicago, Illinois, pp. 991-995.

Assunção, E., 2000, "Redução H_2 e H_∞ de Modelos através de Desigualdades Matriciais Lineares: Otimização Local e Global" , Tese de Doutorado, UNICAMP, Campinas, SP.

Bueno, D. D., 2007, "Controle Ativo de Vibrações e Localização Ótima de Sensores e Atuadores Piezelétricos", Dissertação de Mestrado (Engenharia Mecânica) – Faculdade de Engenharia, Universidade Estadual Paulista, Ilha Solteira.

Boyd, S., Balakrishnan, V., Feron, E. El Ghaoui, L., 1994, "Linear Matrix Inequalities in Systems and Control Theory", Siam Studies in Applied Mathematics, USA, 193p.

Damien, G., 2003, "Circuit Magnétique – Électroaimant" e-LEE, e-learning for Electrical Engineering, http://www.lei.ucl.be/multimedia/eLEE/FR/realisations/CircuitsElectriques/index.htm.

Fuller, C. R., Elliot, S. J., Nelson, P. A., 1996, "Active Control of Vibration", Academic Press.

Gawronski, W., 1998, "Dynamics and Control of Structures: A Modal Approach", 1.ed. New York: Springer Verlag, 231p.

Hansen, C. H., Snyder, S. D., 1997, "Active Control of Noise and Vibrations", E&FN Spon, London UK.

Hutchison, J. R., 2001, "Shear Coefficients for Timoshenko Beam Theoty"; Journal of Applied Mechanics, January.

Juang, J., Phan, Q., 2001, "Identification and Control of Mechanical System", Cambridge University Press, ISBN 0521783550.

Kasarda, M. E., Marshall, J., Prins, R., 2007, "Active magnetic bearing based force measurement using the multi-point technique", Mechanics Research Communications, vol. 34, pp. 44-53.

Koroishi, E. H., Perini, E. A., Nasicmento, L. P., Lopes Jr, V., Steffen Jr, V., 2009, "Modal Active Vibration Control in Rotor System Using Magnetic Bearings with H_∞ norm", Proceedings of the 1rst International Congress of Mathematics, Engineering and Society - ICMES 2009.

Lalanne, M and Ferraris, G. 1997, "Rotordynamics Prediction in Engineering", 2nd edition, Jhon Wiley and Sons, New York.

Liu, F., Zhang, L., 2000, "Modal-Space Control of Flexible Intelligent Truss Structures via Modal Filters:, Proceeding of IMAC – International Modal Analysis Conference, p. 187-193.

Morais, T. S., Steffen Jr, V., Mahfoud, J., Der Hagopian, J., 2009, "Monitoring Cracked Shaft by Using Active Electro-Magnetic Actuator – Numerical Simulation", Proceedings of 20th International Congress of Mechanical Engineering – COBEM 2009.

Palhares, R. M., 1998, "Filtragem Robusta: Uma Abordagem por Desigualdades Matriciais Lineares", Tese de Doutorado, UNICAMP, Campinas, SP.

Saldarriaga. M. V., 2007, "Atenuação de Vibrações em Máquinas Rotativas Flexíveis usando Materiais Viscoelásticos nos Suportes". 111p. Tese de Doutorado. Universidade Federal de Uberlândia, Uberlândia.

Silva, S., Lopes Jr, V., Assunção, E., 2004, "Robust Control to Parametric Uncertainties in Smart Structures Using Linear Matrix Inequalities", Journal of the Brazilian Society of Mechanical Science and Engineering, vol. XXVI, Nº 4, pp. 430-437.

Simões, R. C., 2006, "Controle Modal Ótimo de um Rotor Flexível Utilizando Atuadores Piezelétricos do Tipo Pilha", Tese de Doutorado, Universidade Federal de Uberlândia, Uberlândia, 133p.

Van Antwerp, J. G., Braatz, R. D., 2000, "A Tutorial on Linear and Bilinear Matriz Inequalities", Journal of Process Control, vol. 10, pp. 363–385.

Wang., H. B., Wang, J. L., Lam J., 2007, "Robust Fault Detection Observer Design: Iterative LMI Approaches", Journal of Dynamic Systems, Measurement, and Control, vol. 129, ed. 1, pp. 77-82.

9. RESPONSIBILITY NOTICE

The authors are the only responsible for the printed material included in this paper.